THE ASTROPHYSICAL JOURNAL, 221:731–744, 1978 May 1

DYNAMICAL EVIDENCE FOR A CENTRAL MASS CONCENTRATION IN THE GALAXY M87

W. L. W. SARGENT* AND PETER J YOUNG
Hale Observatories, California Institute of Technology, Carnegie Institution of Washington
A. BOKSENBERG*† AND KEITH SHORTRIDGE*
Department of Physics and Astronomy, University College London
C. R. LYNDS
Kitt Peak National Observatory
AND
F. D. A. HARTWICK*
Department of Astronomy, University of Victoria
Received 1977 September 26; accepted 1977 November 1

ABSTRACT

The elliptical galaxies NGC 3379 (E1) and M87 (E0) have been observed spectroscopically with the University College London Image Photon Counting System. Analysis of the redshifts and velocity dispersions as a function of radius by a Fourier method has yielded the following results: (*a*) NGC 3379 exhibits slight rotation ($v_\theta = 15$ km s^{-1} at $r = 14''$) along the N-S direction (22° from the minor axis). The velocity dispersion is 195 km s^{-1} for $r < 14''$; this shows a small decrease with increasing radius. The data, including the photometric profile, is adequately fitted by a King model with $\log r_T/r_c = 2.20$ and constant $M/\mathscr{L} = 6$ for $0'' < r < 14''$ (with $r_c = 2''.8$). (*b*) M87 shows no rotation ($v_\theta < 10$ km s^{-1}) for $r < 72''$ in the E-W direction. The velocity dispersion at the edge of the core ($r_c = 9''.6$) is 278 km s^{-1}, but decreases to 230 km s^{-1} when $r = 72''$. Inside the core a sharp increase is observed, up to 350 km s^{-1} at $r = 1''.5$. The photometric profile and velocity dispersion data outside the core are explained by a King model with $M/\mathscr{L} = 6.5$ and $\log r_T/r_c = 2.10$. The data inside the core radius can be explained by a central mass concentration $M = 5 \times 10^9\ M_\odot$ contained within $r = 1''.5$ (=110 pc). For $r < 1''.5$ we find $M/\mathscr{L} = 60$, a factor of 10 higher than that in the outer regions. The observed width (1500 km s^{-1} full width at zero intensity) of the [O II] λ3727 doublet also suggests a central mass of $\sim 5 \times 10^9\ M_\odot$.

We conclude that the observations of M87 are entirely consistent with the presence of a central black hole of $\sim 5 \times 10^9\ M_\odot$.

Subject headings: black holes — galaxies: individual — galaxies: internal motions — galaxies: nuclei — galaxies: redshifts

I. INTRODUCTION

The introduction of linear, two-dimensional detectors has at last made it possible to measure accurate velocity dispersions and redshifts in the outer parts of elliptical galaxies, even in regions where the surface brightness is appreciably below that of the sky. As a result, several topics of current theoretical interest have become amenable to observational study. Perhaps the most important among these are (*a*) the search for evidence for supermassive black holes in the centers of elliptical galaxies, particularly in giant ellipticals in which the presence of such objects has been invoked in order to explain explosive or other nonthermal phenomena, (*b*) studies of the rotation curves and radial variation of velocity dispersion in flattened ellipticals in order to check the hypothesis that such systems are supported by rotation, and (*c*) studies of the radial variation of mass and mass-to-light ratio to investigate whether or not galaxies have massive halos.

In a previous paper (Young *et al.* 1978*a*) the first results of our observational program on elliptical galaxies with the two-dimensional version of the University College London image photon counting system (IPCS) were discussed. The rotation curve and velocity dispersion of the E5 galaxy NGC 4473 were measured out to a radius of 45″ (3.3 kpc) from the center. Here we describe similar measurements for the E1 galaxy NGC 3379 and the E0 galaxy M87 (NGC 4486).

As we shall show in later sections, our results for

* Visiting Astronomers, Kitt Peak National Observatory, which is operated by Associated Universities for Research in Astronomy, Inc., under contract from the National Science Foundation.

† Guest Investigator, Hale Observatories.

NGC 3379 and M87 are strikingly different. Consequently, we shall employ NGC 3379 as an example of a normal elliptical galaxy and a standard of comparison for the remarkable behavior of M87. In § II we describe the observations of the two galaxies. The data reduction procedures are described in § III. The spectra were analyzed by a Fourier method due to Sargent *et al.* (1977, henceforth SSBS) which is outlined in § IV. This section also contains the results of the Fourier analysis. Extensive tests of the Fourier method are contained in § V. In § VI we compare the measurements made in the galaxies with models. A model-independent analysis is described in § VII. In § VIII we describe a procedure (also model independent) by which to obtain the mass-to-light ratio as a function of radius. The results are summarized and briefly discussed in § IX.

II. OBSERVATIONS

a) M87

The IPCS was attached to the White spectrograph at the Cassegrain focus of the Kitt Peak 4 m telescope in 1976 April. The slit size was 1″ by 102″; the scale at the Cassegrain focus is 6.″56 mm^{-1}. The IPCS was used in a mode in which 20 spectra (hereafter referred to as "scans") were accumulated simultaneously, equally spaced along the slit. (A complete set of scans will later be referred to as a frame.) Each spectrum was observed with 1000 channels covering 1060 Å along the direction of dispersion. The spatial resolution along the slit was 5.″4. The 1″ slit projected onto two channels on the detector. In order to mount the IPCS on the spectrograph, it was necessary to remove part of the mu-metal shield around the focusing coil of the electromagnetically focused image tube. As a result the spectra obtained with this arrangement suffered from severe S-distortion. Consequently, as mentioned in § II, it was sometimes necessary to reject data at either end of the spectrum. Also, the focus was inferior to that normally obtained with the device. Careful attention was paid to make observations of the object, the sky, and standard comparison stars under identical operating conditions.

A complete journal of observations made in connection with M87 is given in the first part of Table 1. Observations on the galaxy were made with the slit E-W and placed at various positions relative to the nucleus of the galaxy. Particular care was taken to avoid the region of the optical "jet." The furthest extent of the slit from the center of M87 was 150″. As indicated in Table 1, extensive exposures to measure the sky background were made on an area free of visible stars 1° S of M87. An inert gas wavelength comparison source (containing He, Ne, Ar, and Kr) was recorded frequently. Three bright comparison stars were observed for use in conjunction with the Fourier method used to measure radial velocities, line strengths, and velocity dispersions. These were HR 5709 (K0 III), HR 5741 (K4 III), and HR 5888 (G8 III). Five magn. neutral density filters were inserted during the observations of the stars in order to obtain acceptable counting rates with the IPCS. Further details pertinent to the M87 observations are given in Table 1.

b) NGC 3379

Observations of NGC 3379 were made with the IPCS at the coudé focus of the 5 m Hale telescope in 1977 April. The device was attached to the 36 inch (91 cm) camera in the manner described by Boksenberg and Sargent (1975). As at Kitt Peak the IPCS was operated in a two-dimensional mode in which 17 spectra (scans) were recorded simultaneously, each

TABLE 1

JOURNAL OF OBSERVATIONS FOR M87 AND NGC 3379

Raw Data Set No.	Object	Night	Slit p.a.	Slit* Position	Spectral Coverage (Å)	Bin Size (Å)	Resolution FWHM (Å)	Time on Object (sec)	Time on Sky (sec)
1	M87	1 Apr 1976	90°	0"	3799-4863	1.06	4.6	2600	0
2	M87	1 Apr 1976	90°	102"E	3799-4863	1.06	4.6	5000	0
3	HR 5709	1 Apr 1976	90°	0"	3799-4863	1.06	4.6	617	...
4	HR 5741	1 Apr 1976	90°	0"	3799-4863	1.06	4.6	1000	...
5	M87	3 Apr 1976	90°	51"W	3631-4696	1.07	4.6	3000	1800
6	M87	3 Apr 1976	90°	102"W	3631-4696	1.07	4.6	9600	4800
7	HR 5709	3 Apr 1976	90°	0"	3631-4696	1.07	4.6	600	...
8	HR 5741	3 Apr 1976	90°	0"	3631-4696	1.07	4.6	513	...
9	HR 5888	3 Apr 1976	90°	0"	3631-4696	1.07	4.6	513	...
10	NGC 3379	12 Apr 1977	0°	0"	3985-4296	0.31	0.74	10500	1500
11	HD 92706	12 Apr 1977	0°	0"	3985-4296	0.31	0.74	910	...
12	HR 4207	12 Apr 1977	0°	0"	3985-4296	0.31	0.74	400	...

*This column gives the position of the center of the slit relative to the nucleus of the object.

containing 1000 channels spread over 310 Å in wavelength. The scale at the coudé focus is 1".2 mm^{-1}, and the observations were made with a slit 1" wide and 40" long. The slit width projected to 2 channels on the detector. The spatial resolution along the slit was 2".4. All observations of NGC 3379 were made with the nucleus of the galaxy at the center of the slit. A complete journal of observations made in connection with NGC 3379 is given in the bottom part of Table 1. Sky exposures were made on an area 5' N of the nucleus. Frequent observations were also made of a hollow cathode Ar-Fe comparison arc. Two bright K giant stars were observed for use in conjunction with the Fourier analysis of the galaxy data. These were HD 92706 (gK2) and HR 4027 (gK1). Neutral density filters were used to cut down the counting rate to an acceptable level during the stellar observations. Further pertinent details of the NGC 3379 observations are given in Table 1.

c) *Flat Fields*

In order to correct for small-scale variations in sensitivity of the IPCS, observations were made at both Kitt Peak and Palomar of flat fields. For this purpose, at both observatories a diffuse incandescent lamp was observed through the spectrograph slit. At Kitt Peak observations were also made of the comparison arc with a diffuse Mylar screen in place of the grating in the spectrograph. The flat fields were used in the reductions described in the following section.

III. DATA REDUCTION

The reduction procedure was standardized for all sets of data and consisted of the following steps:

1. All frames (including arcs) were divided by an appropriate flat-field frame:

$$N'(i,j) = N(i,j)/F(i,j) \qquad (1 \le i \le 1000;\ 1 \le i \le j_{\max}),$$
$$\langle F(i,j)\rangle_{ij} = 1, \qquad (1)$$

where i is the channel number, j is the scan number, and $j_{\max}$ is the total number of scans in a frame (20 for M87 and 17 for NGC 3379).

2. The drifts in the arc lines from frame to frame were scrutinized, and the data broken into sets within which the drifts were less than 0.25 channels. The arcs in each of the resulting sets were summed; and 24 strong, unblended lines were chosen by trial and error to establish a wavelength scale for each scan within a frame by the following least squares procedure. Arc lines of tabulated wavelength λ_k were established to be at positions $N_k(j)$ $(1 \le j \le j_{\max})$ in each scan and at a mean position $N_k = \langle N_k(k)\rangle_j$. A least squares procedure on ϵ_k determined the coefficients α_i in the following relations:

$$N_k + \epsilon_k = \sum_{i=0}^{3} \alpha_i \lambda_k{}^i . \qquad (2)$$

Then a least squares minimization of $\zeta_k(j)$ determined the b_{mn} in the subsequent approximation,

$$N_k(j) - \sum_{i=0}^{3} \alpha_i \lambda_k{}^i + \zeta_k(j) = \sum_{m=0}^{2}\sum_{n=0}^{2} b_{mn}\lambda_k{}^m j^n . \qquad (3)$$

Wavelength λ was then considered to be at a position

$$N(\lambda, j) = \sum_{l=0}^{3} \alpha_l \lambda^l + \sum_{m=0}^{2}\sum_{n=0}^{2} b_{mn}\lambda^m j^n . \qquad (4)$$

The deviation of a single arc line was typically 0.3 channels, and so the wavelength scale may be expected to have an internal accuracy of $\sim$0.05 channels.

3. The data were rebinned into 1024 channels on a logarithmic scale by linear interpolation among the original channels. If the new channel overlaps with fraction f_i of the old channel i (containing N_i counts), then

$$N_{\text{new}} = \sum_{i=1}^{1000} f_i N_i ; \qquad \sum_{i=1}^{1000} f_i = 1 . \qquad (5)$$

4. When sky frames S_k were observed, the sky subtraction was performed by linear subtraction of the sum of the sky frames from the sum of the galaxy frames G_k:

$$G'(i,j) = \sum_{k=1}^{n_G} G_k(i,j) - (T_G/T_s) \sum_{k=1}^{n_s} S_k(i,j) , \qquad (6)$$

where T_G is the total integration time on the galaxy and T_s is the time on the sky. For the standard stars, sky was subtracted by an equivalent procedure using the scans not containing the star. For the M87 data sets 1 and 2 in Table 1, the sky was not observed. In these cases the scans covering the outer part of the galaxy were used as "sky" for the scans covering the inner part. In particular, for data set 2 taken 102" E of the center of M87, "object" scans were deemed to be $j = 1$ to 8, and "sky" scans $j = 9$ to 16. For reasons to be discussed in § V, such data are to be given low weight when the sky is comparable in brightness to the galaxy.

5. As already mentioned, the M87 data were affected by severe S-distortion. Where the extent of the distortion was less than 0.2 scans, a two-dimensional linear rebinning procedure was used to straighten the scans. Data with distortions in excess of this at the ends of the spectra were not included in the analysis. Table 2 lists the actual wavelength range used.

6. The standard star frames for a particular star were added together when observations on more than one night existed, so as to give the highest possible quality spectra for the Fourier analysis.

Experience has shown that galaxy spectra require at least a total of 10^5 counts, and preferably 3×10^5 counts, for the Fourier analysis. To achieve this, adjacent scans were added where necessary. The position of such a summation of scans from j_1 to j_2

TABLE 2

M87 AND NGC 3379: REBINNED DATA PARAMETERS

Rebinned Set No.	Raw Data Set No.	Object	Slit p.a.	Slit Position	Spectral Coverage (Å)	Bin Size (km s^{-1})	Resolution FWHM (km s^{-1})	Total No. of Counts on Orbit ($N/10^5$)
1	1	M87	90°	0"	3805-4670	60	330	35.0
2	2	M87	90°	102"E	3805-4670	60	330	2.7
3	5	M87	90°	51"W	3805-4670	60	330	17.3
4	6	M87	90°	102"W	3805-4670	60	330	4.1
5	3,7	HR 5709	90°	0"	3805-4670	60	330	11.5
6	4,8	HR 5741	90°	0"	3805-4670	60	330	14.6
7	9	HR 5888	90°	0"	3805-4670	60	330	7.7
8	10	NGC 3379	0°	0"	4000-4283	20	53	21.0
9	11	HD 92706	0°	0"	4000-4283	20	53	14.6
10	12	HR 4207	0°	0"	4000-4283	20	53	6.6

was deemed to be at a luminosity-weighted average position:

$$\langle j \rangle = \sum_{j=j_1}^{j_2} jN_G(j) \Big/ \sum_{j=j_1}^{j_2} N_G(j)\,, \qquad (7)$$

where $N_G(j)$ is the total number of counts in scan j.

Table 2 gives the relevant parameters and details of the various sets of rebinned data for M87 and NGC 3579.

IV. FOURIER ANALYSIS AND RESULTS

In Figure 1 we display spectra of a comparison star, of the outer region ($r = 70''$) of M87, and also of the nucleus of M87. The differences in the line widths are striking, particularly when comparing the two M87 spectra. A detailed examination suggests that the velocity dispersion in the outer regions of M87 is much lower than in the nucleus. Differences in structure around the G band, and the Ca II H and K lines, are also evident. A rough measurement of the line widths gives values $\sigma(r = 70'') \sim 200$ km s^{-1} and σ(nucleus) ~ 300 km s^{-1} for M87. We note, however, that visual techniques for determining velocity dispersions are less reliable than Fourier methods. As SSBS have shown in detail, direct analyses of the data in wavelength space have difficulties in differentiating between line strengths and line widths.

In the Fourier method described by SSBS, the

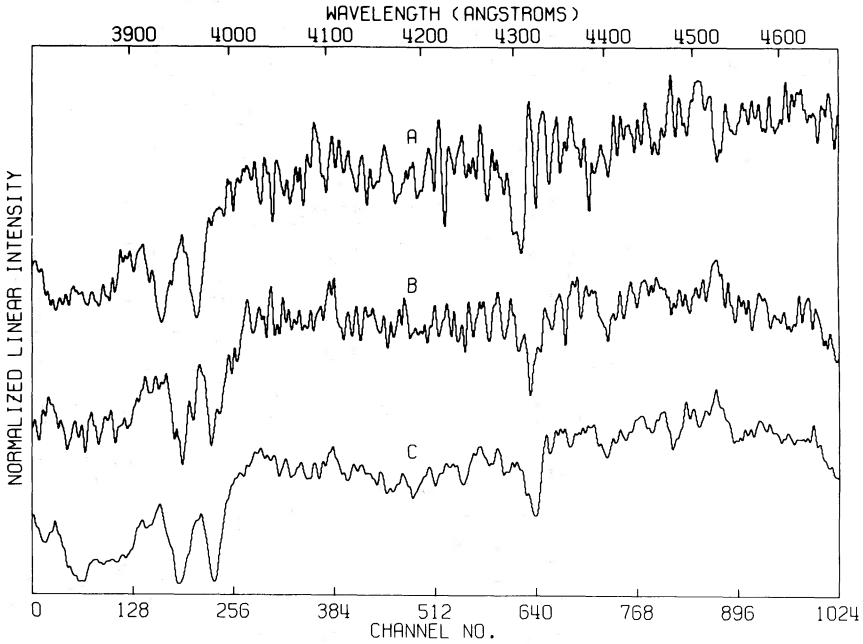

FIG. 1.—IPCS spectra of (*A*) comparison star HR 5709 (K0 III), (*B*) M87 at a distance of 70″ W of the center, (*C*) M87 4″ E of center. Note the broad, shallow lines of spectrum *C* as compared with *B*. The Fourier velocity dispersions were $\sigma_v = 220$ km s^{-1} for *B* and 300 km s^{-1} for *C*.

discrete Fourier transforms of the galaxy and star spectra $\tilde{G}(k)$ and $\tilde{S}(k)$, respectively, are evaluated. The quotient $Q(k) = \tilde{G}(k)/\tilde{S}(k)$ is then compared by a least squares fit to the broadening function

$$B(k) = \gamma \exp\left[-\frac{1}{2}\left(\frac{2\pi k\sigma_v}{nc\Delta \ln \lambda}\right)^2 + \frac{2\pi i k \ln(1+z)}{n\Delta \ln \lambda}\right], \quad (8)$$

to determine simultaneously the redshift z, the velocity dispersion σ_v, and the relative line strength γ. Here n is the number of real space channels, and $\Delta \ln \lambda$ the channel width. A weighting function for the least squares analysis is obtained by estimating the standard deviation $\Delta Q(k)$ in the quotient $Q(k)$ and then minimizing

$$\chi^2 = \sum_{k=k_L}^{k_H} \left|\frac{Q(k) - B(k)}{\Delta Q(k)}\right|^2,$$

where k_H and k_L are the upper and lower limits of the domain in Fourier space to be fitted. In previous versions of this analysis an evaluation of the noise level in the data was used to choose a value of k_H (k_L was fixed). To ensure uniformity we have kept k_H fixed for each galaxy. Thus, for M87 we used $k_L = 5$ and $k_H = 80$, while for NGC 3379 we used $k_L = 10$ and $k_H = 40$. As was demonstrated by SSBS, the results do not depend on k_H to any significant degree.

The Fourier analysis procedure described above was carried out for the data on both galaxies. First we discuss the results obtained for NGC 3379. These are given in Figure 2 and Table 3, and are the mean of the values obtained with the two comparison stars listed in Table 1. The spectrograph slit was oriented N-S on this E1 galaxy, at an angle of 22° to the minor axis (the position angle of the major axis is 68° [Dennison 1954, as quoted by de Vaucouleurs 1959]). The core radius of the galaxy is $r_c = 2''.8 \pm 0''.3$ from photometry by Kormendy (1977) and by Young *et al.* (1978*c*). The distance to NGC 3379 is $\Delta = 8$ Mpc (de Vaucouleurs 1975), but we shall include a distance factor $\delta_8 = \Delta/8$ Mpc in all relevant quantities without including possible errors in δ_8 when estimating errors.

Our values for the mean redshift and velocity dispersion of NGC 3379 are $cz = 905 \pm 16$ km s^{-1} and $\sigma_v = 195 \pm 17$ km s^{-1}, respectively. These may be compared with previously published values of $cz = 885 \pm 27$ km s^{-1} (de Vaucouleurs, de Vaucouleurs, and Corwin 1976) and $\sigma_v = 240 \pm 40$ km s^{-1} (Faber and Jackson 1976), 187 ± 6 km s^{-1} (Burbidge, Burbidge, and Fish 1961), 125 km s^{-1} (de Vaucouleurs 1974), 133 ± 20 km s^{-1} (Williams 1977), and 187 km s^{-1} (Minkowski 1962). As usual, the results for σ_v range over nearly a factor of 2; these reflect systematic differences between the various methods of analysis. The Fourier method described here has been subject to extensive tests (see SSBS); further tests will be described in § V. We thus are confident that the results are free from systematic errors of more than 10%.

Reference to Figure 2 shows a slight rotational tilt

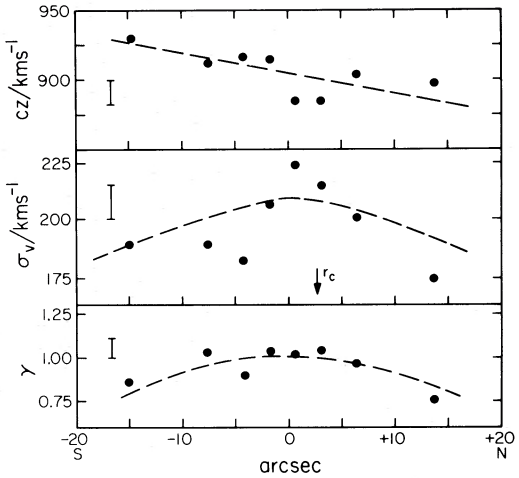

FIG. 2.—Results for NGC 3379. The redshift (cz), velocity dispersion (σ_v) and relative line strength (γ) of galaxy and comparison star were found simultaneously by Fourier methods. The core radius of the galaxy, $r_c = 2''.8$, is marked. Error bars of length 2 σ are given.

in the plot of redshift as a function of radius, even at an angle of 22° to the minor axis. We find a rotation speed of 1.5 ± 0.5 km s^{-1} arcsec^{-1} with the N side of the galaxy approaching. Correction to the major axis would give 4.0 ± 1.3 km s^{-1} arcsec^{-1}.

The velocity dispersion shows a slight decrease away from the center; this was also found by Faber and Jackson (1976), who found $\sigma_v = 210 \pm 20$ km s^{-1} at a distance of $r = 10''$. The line strength parameter γ also seems to show a slight decrease away from the center.

We next consider the results for M87. These are given in Table 3 and displayed in Figures 3 and 4. M87 is classified as an E0 galaxy, and the isophotes in the central regions are accurately circular (Young *et al.* 1978*b*). The core radius is $r_c = 9''.6 \pm 0''.5$, and the distance is $\Delta = 13.6$ Mpc (de Vaucouleurs 1975) or $\Delta = 19.5$ Mpc (Sandage and Tammann 1974). We shall adopt $\Delta = 15$ Mpc and include a quantity $\delta_{15} = \Delta/15$ Mpc in later computations.

The mean values for the redshift and velocity dispersion of M87 are $cz = 1287 \pm 21$ km s^{-1} and

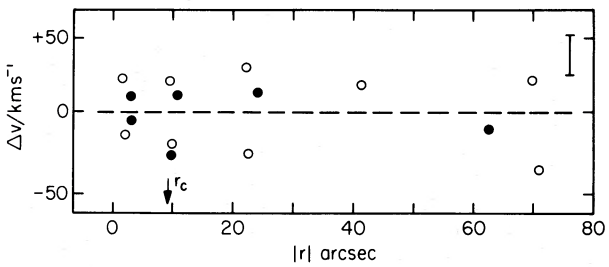

FIG. 3.—Rotational velocities of M87. The open circles (○) are points to the W of the nucleus for which $\Delta v = cz - \langle cz \rangle$ has been plotted; the filled circles (●) are to the E for which $-\Delta v$ has been plotted. The core radius of the galaxy, $r_c = 9''.6$, is marked. A 2 σ error bar is given.

TABLE 3

M87 AND NGC 3379: REDSHIFTS, LINE STRENGTHS, AND VELOCITY DISPERSIONS

Object	Data Set From Table 2	Scan Block	$N_G/10^5$	$\langle r" \rangle$*	$\langle cz \rangle$† (km s^{-1})	$\langle \gamma \rangle^{\neq}$	$\langle \sigma_v \rangle$ (km s^{-1})
M87	1	5-7	3.2	-22.1	1314±16	0.96±0.03	260±17
	1	8-9	6.2	- 9.2	1305±15	1.00±0.03	295±16
	1	10	7.3	- 1.6	1306±20	0.95±0.03	329±21
	1	11	6.7	+ 3.8	1293±20	0.95±0.03	333±21
	1	12-13	5.3	+11.3	1277±16	1.03±0.03	275±16
	1	14-16	3.1	+24.3	1276±17	0.99±0.03	287±18
	2#	1-8	2.7	+62.2	1297±50	0.81±0.08	258±64
	3	1-7	0.9	-69.7	1306±39	0.75±0.07	189±48
	3	8-11	1.2	-41.6	1304±25	0.97±0.05	268±29
	3	12-14	2.0	-22.7	1259±20	0.99±0.04	280±21
	3	15-16	3.5	- 9.7	1267±16	1.09±0.03	301±17
	3	17	3.9	- 2.2	1273±23	1.05±0.04	362±26
	3	18	3.6	+ 3.2	1275±20	1.01±0.04	321±22
	3	19-20	2.2	+ 9.7	1314±18	1.02±0.04	286±19
	4	1-20	4.1	-71.8	1250±21	0.86±0.04	232±23
Mean Value					1287±21		278±11§
NGC 3379	8	1-4	1.7	-14.2	930±25	0.86±0.18	189±33
	8	5-6	1.9	- 7.4	911±13	1.03±0.11	188±18
	8	7	2.0	- 4.1	916±16	0.90±0.11	181±21
	8	8	3.9	- 1.7	913±13	1.04±0.11	206±16
	8	9	4.7	+ 0.7	883±18	1.02±0.12	223±21
	8	10	2.5	+ 3.1	883±16	1.04±0.10	214±16
	8	11-12	2.2	+ 6.5	903±18	0.97±0.13	200±22
	8	13-17	2.1	+13.9	899±18	0.76±0.11	174±25
Mean Value					905±16		195±17

*Positive values to the E for M87, to the N for NGC 3379

#Questionable data point (sky not observed, see § V).

†Heliocentric

≠ Reduced such that mean value of γ in the region $r < 4r_c$ is unity.

§ Mean value for 10" < |r| < 42" intended to represent the dispersion outside the central spike but not including the gradual drop in the outer regions.

$\sigma_v = 278 \pm 11$ km s^{-1}, where the value for σ_v refers to the region $10'' < r < 42''$. These may be compared with the values of $cz = 1257 \pm 16$ km s^{-1} (de Vaucouleurs, de Vaucouleurs, and Corwin 1976), $\sigma_v = 490 \pm 55$ km s^{-1} (Minkowski 1962), 550 ± 70 km s^{-1} (Brandt and Roosen 1969), and 315 ± 20 km s^{-1} (Faber and Jackson 1976). The older values of σ_v are undoubtedly too high, being measured by visual methods, but our value is consistent with that of Faber and Jackson (1976) when one allows for the fact that their measurements are systematically 22% higher than those of SSBS.

We see from Figure 3 that there is no evidence for rotation along the E-W direction in M87; the velocity amplitude is less than 10 km s^{-1} for $r < 72''$. This is not surprising considering the circularity of the central isophotes and the low rotation velocities found in flattened elliptical systems (Bertola and Capaccioli 1975; Young *et al.* 1978*a*).

The velocity dispersion varies with radius, as was suspected from a crude examination of the spectra in Figure 1 of the sharpness of the spectral lines. It falls from $\sigma_v = 350$ km s^{-1} at $r = 1''.5$, to $\sigma_v = 220$ km s^{-1} at $r = 72''$. Outside the core radius the variations of σ_v are gradual, but inside the core radius the value of σ_v rises rapidly, as may be seen from Figure 4. The data have not been corrected to allow for seeing or resolution effects; were this to be done, the central

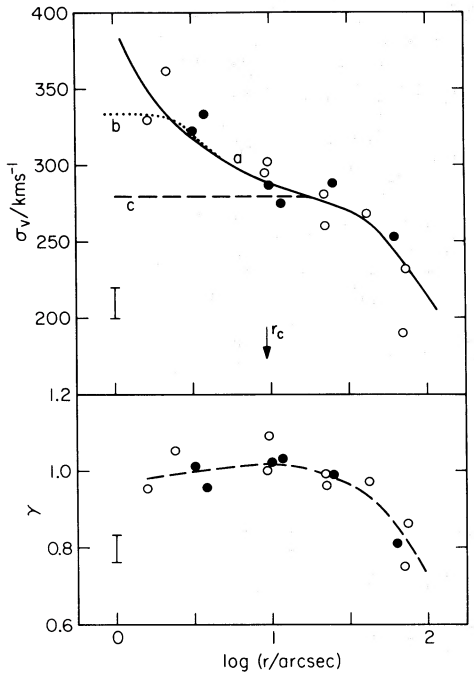

FIG. 4.—Velocity dispersions (σ_v) and the line strengths (γ) for M87. The open circles (○) are points W of the nucleus, and the filled circles (●) are E. The core radius, $r_c = 9''.6$, of the galaxy is marked. Error bars of length 2σ are given. Curve (*a*) is the velocity dispersion predicted by the black hole model fitted to the photometric data, (*b*) is the same model convolved with the seeing disk and slit size for the spectroscopic observations, and (*c*) is the King model that would prevail if the black hole were absent.

increase would be even more pronounced. (In § VI we shall allow for such effects when fitting models to the data.) The decrease in the line strength γ away from the nucleus is also notable. Such an effect was found in NGC 3379 and also in NGC 4473 (Young *et al.* 1978*a*). However, the line strength γ shows only a very slight drop as $r \to 0$, in the nuclear regions themselves; for $r < r_c$ we find $\Delta\gamma/\gamma \leq 0.04$. This observation places a limit on the amount of nonthermal blue radiation emitted by the central bright nucleus, this limit being 20% of the light emitted inside the central $1''.5$ radius (see Young *et al.* 1978*b*).

Figure 5 shows spectra of the nucleus and of the immediately adjacent regions of M87. The slightly greater velocity dispersion of the nucleus (350 km s^{-1} as opposed to 320 km s^{-1} in the other spectra) manifests itself as slightly broader lines. There are slight differences in structure (for example, in the Fe lines around 4700 Å) in the central spectrum, but there is certainly no filling in of the Ca II H and K lines as is observed in the region of the jet.

V. FURTHER TESTS OF THE FOURIER METHOD

The Fourier method as described and used here was exhaustively tested by SSBS. Their conclusions may be summarized as follows:

1. The Fourier method gave results in agreement with visual techniques involving artificial broadening of the stellar lines.

2. Artificial "galaxy" spectra were obtained by convolving a template star with a Gaussian broadening function. These yielded the correct values for the

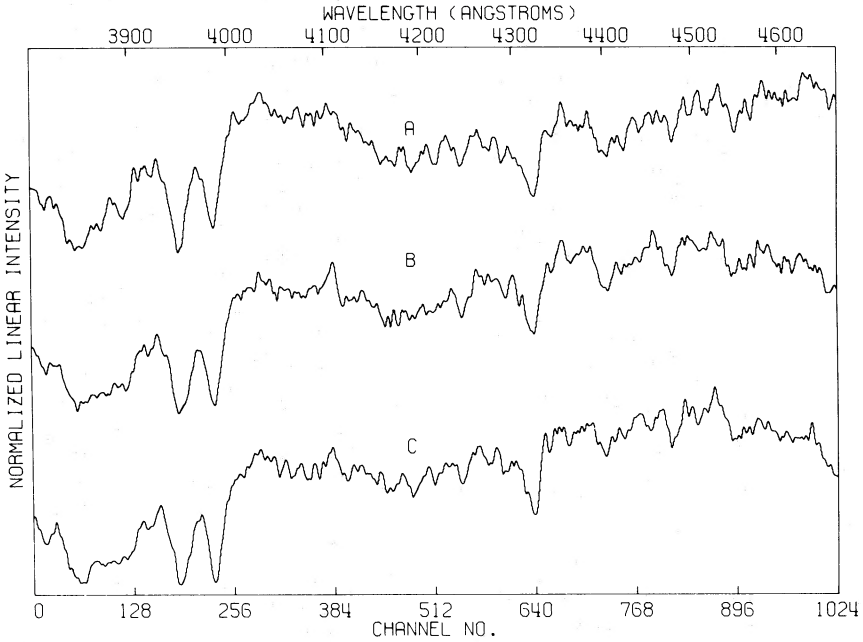

FIG. 5.—IPCS spectra of M87. (*A*) 9″ W of center, (*B*) 2″ W of center, (*C*) 4″ E of center. The velocity dispersions found from Fourier analysis were σ_v = 300 km s^{-1}, 350 km s^{-1}, and 325 km s^{-1}, respectively; this is in accord with the line widths by visual inspection. The line strengths vary by less than 4% in these three spectra.

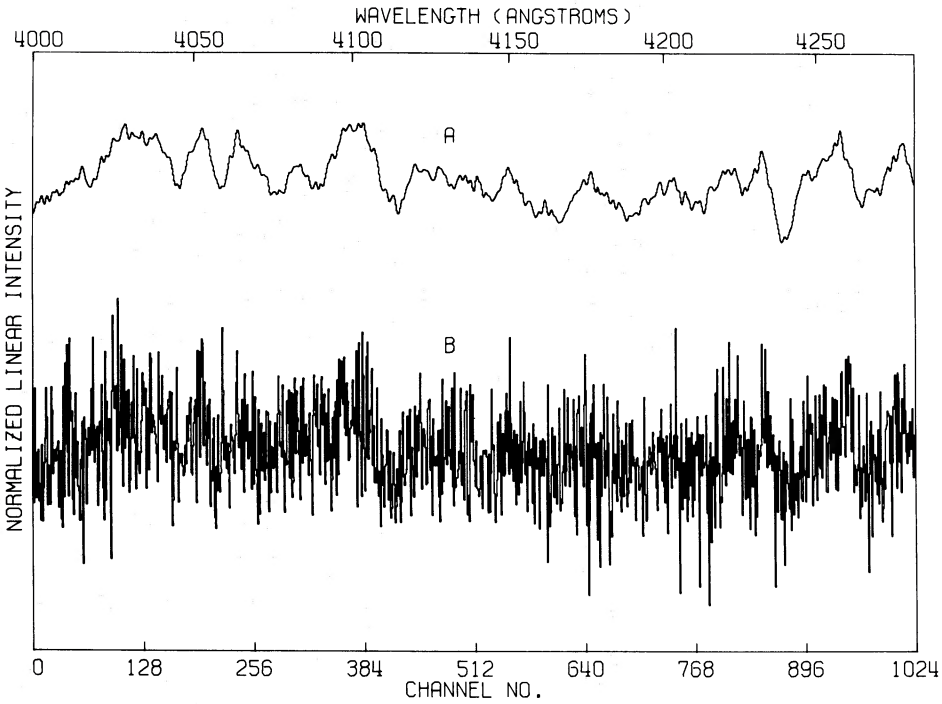

FIG. 6.—(*A*) IPCS spectrum of NGC 3379, (*B*) the same spectrum with the noise level artificially enhanced. The Fourier analysis found velocity dispersions for these two spectra differing by only 2 km s^{-1}.

broadening parameters when tested against a second star.

3. Different spectral regions gave the same results for σ_v.

4. Using composite template spectra (or using M32) did not change the results.

5. Differing regions of Fourier space gave identical results.

In the present work we have extended the use of the Fourier method to the faint, outer parts of galaxies. Accordingly, we have made further tests:

1. The spectra for M87 contain the Ca II H and K lines. Since these are the strongest features and are on the square root part of the curve of growth, changes in metallicity will affect these lines differently from the weaker ones. That this effect is small and does not bias the σ_v results has been tested by performing reductions on the spectra excluding the H and K lines. No significant difference was apparent.

2. The effect of differing signal-to-noise ratios in the various spectra was tested by artificially adding noise with a random number generator. Figure 6 shows a (smoothed) test spectrum of NGC 3379 together with a severely degraded version. A succession of such degraded spectra with progressively greater noise was analyzed by the SSBS Fourier method to obtain a series of cz, γ, σ_v values. In Figure 7 these are plotted against the effective numbers of photon counts in the galaxy spectrum, N_G, required to produce the various noise levels, assuming photon statistics. The results in Figure 7 show that there is no systematic deviation with varying N_G, and that the two spectra in Figure 6 yield values of σ_v differing by only 2 km s^{-1}! All the results in this paper were based on $N_G > 10^5$, and most have $N_G > 3 \times 10^5$.

3. Similar tests were made by adding random noise to template star spectra. Here results are different. The method failed when N_S became $\lesssim 5 \times 10^5$, particularly if the galaxy spectrum was itself rather noisy. This is to be expected since we divide by $\tilde{S}(k)$, the Fourier transform of the star spectrum, and so fluctuations of $\tilde{S}(k)$ toward zero will have a large effect on the ratio $\tilde{G}(k)/\tilde{S}(k)$.

4. The results obtained in tests (2) and (3) lead us to recommend that: (*a*) Template stars should have at least $N_s = 10^6$ counts in the whole spectrum. (*b*) Given high-quality template star spectra, acceptable results for the galaxies can be obtained with $N_G = 10^5$ photons; however, $N_G \gtrsim 3 \times 10^5$ counts is preferable.

5. A central blue "continuum" source may be present in the nucleus of M87 (Young *et al.* 1978*b*). This may be nonthermal synchrotron emission, or merely a cluster of early-type stars. To test whether this would bias the velocity dispersion results, a noisy continuum level was added to selected spectra. The Fourier method successfully extracted the correct cz, γ, and σ_v values even when this added continuum was 10 times as big as the galaxy continuum. We are therefore confident that such a blue continuum cannot bias the results for the velocity dispersion near the center of M87.

6. The effects of a contaminating sky spectrum were tested by adding sky and its derivative (to

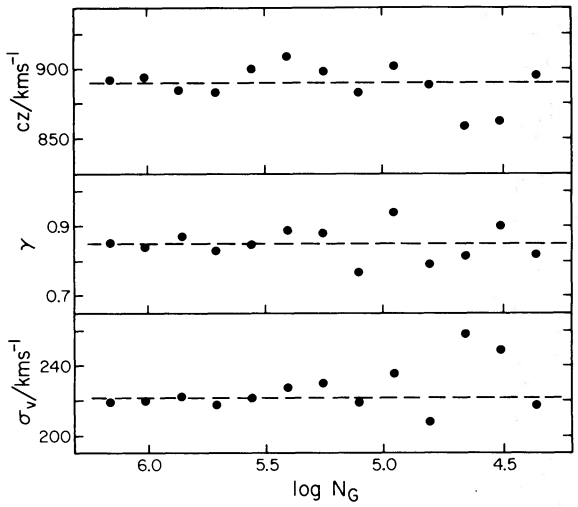

FIG. 7.—Results of tests on an artificially degraded spectrum of NGC 3379. The noise level was enhanced to simulate real data with a total of N_G photons counted in the whole spectrum. The Fourier method was used to find redshifts (cz), line strengths (γ), and velocity dispersions (σ_v) for this series of spectra. No systematic trend in the results is evident, demonstrating the insensitivity of the method to signal-to-noise ratio.

simulate slightly misbinned sky subtraction) to one of the M87 spectra. Since the sky contains a solar spectrum from zodiacal light at zero redshift and velocity dispersion, it may be expected to affect the Fourier results. As might be guessed, the addition of "sky derivative" had little effect, but the addition of sky had a very serious effect. This was empirically determined to be:

$$\frac{\Delta\sigma_v}{\sigma_v} \sim \frac{3}{2}\left(\frac{\Delta N_s}{N_s}\right)\left(\frac{N_s}{N_G}\right), \qquad (9)$$

where $\Delta\sigma_v$ is the error induced in σ_v, $(\Delta N_s/N_s)$ is the fractional mis-subtraction of the sky (measured relative to the sky itself, positive for sky, negative for anti-sky) and (N_s/N_G) is the ratio of strength of the sky to that of the galaxy. From equation (9) we see that an error in the sky level of only 20% will perturb σ_v by 70 km s^{-1}. The effect can go either way, depending on the sign of the error.

Accordingly, we have made considerable efforts to ensure that the sky subtraction is correct; we can guarantee it to $\sim$2% ($\Delta\sigma_v \sim 7$ km s^{-1}), having made the following checks: (*a*) The plots of the sky-subtracted galaxy spectra were inspected to ensure that the night-sky emission lines have been correctly removed. (*b*) The various sky frames were subtracted from one another. The photometric stability of the IPCS was checked by scrutiny of the total counts in series of object and sky frames. (*c*) Galaxy and sky frames were cross-correlated to check that no peak was present at the origin.

The check using the night-sky emission lines is not good to better than $\sim$10% but was used to ensure that a gross error had not been made. Inspection of the photometric stability of the counting rates on sky and galaxy suggests expected subtraction errors of $\lesssim$2%. This was the accuracy of the sky intersubtraction tests, further checked using method (*c*). Fortunately the sky subtraction affects only the outermost data points where the sky brightness is comparable with that of the galaxy. Here we have multiple sets of data which are in reasonable agreement with each other. However, the problem with the sky subtraction is the reason for our suspicion of the result obtained from data set 2 (see Table 3).

It is clear from these considerations that velocity dispersion measurements in the outer regions of galaxies must be carried out on dark, photometric nights, and that sky monitoring should be conducted frequently and preferably with a total integration time equal to that spent on the galaxy.

7. The correlation coefficient between the parameters cz, γ, and σ_v were typically found to be $r(cz, \gamma) = 10^{-8}$, $r(cz, \sigma_v) = 10^{-8}$, and $r(\gamma, \sigma_v) = 0.4$. As might be expected, there is a positive correlation between the values of γ and σ_v; this is visible in Figure 7. A fall in the determined value of σ_v is usually accompanied by a fall in γ. On these grounds one might suspect the data for the outer regions of NGC 3379 and M87 where σ_v and γ both decrease. However, the effect would have to be of the order $|\Delta\sigma_v/\sigma_v| \sim 0.25$ in both of the data points for M87 at $r \sim 70''$. We consider this unlikely in view of the evidence of Figure 1 and the stability of the Fourier method which we have demonstrated in the previous sections.

VI. COMPARISON WITH MODELS

We have used the data in Table 3 on the radial variation of σ_v in order to calculate the mass distributions in the two galaxies. We find that in the case of NGC 3379 a theoretical model from the family calculated by King (1966) fits both the photometric data and the dynamical observations reasonably well. However, in the case of M87 a simple theoretical model does not give a satisfactory fit to the data. Consequently, for M87 we have devised a procedure to obtain the mass distribution which is model independent. This will be described in § VII. We first consider the model fits to the two galaxies.

a) NGC 3379

The photometric profile of NGC 3379 is adequately fitted by a King model with $\log r_T/r_c = 2.20$, although there may be a central spike detectable only by deconvolution of the seeing effects (de Vaucouleurs and Capaccioli 1978). The core radius is $r_c = 2''.8 = 109\delta_8$ pc. In Figure 2 we have plotted the predicted variation of σ_v with radius according to this model; it would seem adequate to explain the slight fall in σ_v out to $r = 14''$. This fit suggests that $M/\mathscr{L}$ will be constant for $r \leq 14''$, a question to be examined in more detail in § VIII.

Using the photometric data of Kormendy (1977) and Young *et al.* (1978*c*), we find a central surface

brightness of $\mu_V = 15.85 \pm 0.02$ mag arcsec^{-2} and a core radius $r_c = 2''.8 \pm 0''.3 = (109 \pm 12)\,\delta_8$ pc. Correcting for a galactic absorption of $A_V = 0.14$, we find a projected central luminosity $L_c = (1.9 \pm 0.1) \times 10^4\,L_\odot\,\mathrm{pc}^{-2}$, and a central luminosity $L_\odot = (186 \pm 10)\,\delta_8{}^{-1}\,L_\odot\,\mathrm{pc}^{-3}$. Taking $\sigma_v = 195 \pm 17$ km s^{-1}, the central density $\rho_0 = 9\sigma_v{}^2/4\pi G r_c{}^2 = (515 \pm 105)\,\delta_8{}^{-2}\,M_\odot\,\mathrm{pc}^{-3}$. The central mass-to-light ratio is then $M/\mathscr{L} = (6 \pm 1)\,\delta_8{}^{-1}$.

b) M87

The photometric profile of the outer regions ($20'' < r < 5'$) of M87 may be fitted by a King model with $\log r_T/r_c = 2.10$; however, the center is grossly deviant, with a steep starlike "cusp" (Young *et al.* 1978*b*). An additional blue source exists for $r < 1''.5$. Figure 4 shows that the velocity dispersion data are also inconsistent with any sort of King or isothermal model since there is a sharp central spike inside the core radius. The CCD photometric data of Young *et al.* (1978*b*) has been fitted with a King model containing a central black hole. Parameters of the fit are found to be:

Galaxy core radius:

$$r_c = 9''.6 \pm 0''.5 = (698 \pm 36)\delta_{15}\,\mathrm{pc},$$

Core surface brightness:

$$\mu_V = 17.20 \pm 0.02\ \mathrm{mag\ arcsec}^{-2}.$$

On correcting for a galactic absorption of $A_V = 0.14$ mag, we find

Core surface luminosity:

$$L_c = (5.5 \pm 0.1) \times 10^3\,L_\odot\,\mathrm{pc}^{-2}$$

Core space luminosity:

$$L_0 = (4.0 \pm 0.2)\delta_{15}{}^{-1}\,L_\odot\,\mathrm{pc}^{-3},$$

Core space density: $\rho_0 = (26 \pm 3)\delta_{15}{}^{-2}\,M_\odot\,\mathrm{pc}^{-3}$,

Mass-luminosity ratio of central stellar population:

$$M/\mathscr{L} = (6.5 \pm 0.6)\delta_{15}{}^{-1}.$$

The "core" parameters given above are not those for an isothermal sphere fit since, as we mentioned above, this model does not agree with the observed profile. Rather they are parameters representing the fit of the black hole model and are the values pertinent to the isothermal model that results if the black hole is not present. The value of $M/\mathscr{L}$ is surprisingly small; this is due mainly to the fact that our value of σ_v is down by a factor of 2 on older values. The black hole mass fitted by Young *et al.* (1978*b*) is $M_H = (2.6 \pm 0.5) \times 10^9\,M_\odot$. We have fitted the expected velocity dispersion from this model to the data points in Figure 4, where we see that the agreement is satisfactory. We discuss the presence of a central mass further in § VIII.

VII. THE MASS DISTRIBUTION IN THE CENTER OF M87

a) Further Analysis of $\sigma_v(r)$

It is possible to deduce the mass distribution in M87 on quite general principles which do not depend on fitting specific models. By taking the first moment of the spherical, collisionless Boltzmann equation it is easy to show that:

$$\frac{d}{dr}\left[\rho_*(r)\sigma_v{}^2(r)\right] = -\frac{GM(r)}{r^2}\,\rho_*(r), \qquad (10)$$

where $\rho_*(r)$ is the density of the stars which give rise to the observed luminosity and $\sigma_v(r)$, as before, is the radial component of the velocity dispersion of these same stars. In deriving equation (10) it is assumed that σ_v is isotropic. $M(r)$ refers to the *total* mass inside radius r, not just the mass of the stellar population which radiates the observed light. Equation (10) can easily be transformed into the following expression for $M(r)$:

$$M(r) = \frac{r\sigma_v{}^2(r)}{G} \times \left[-\frac{d\ln L_*}{d\ln r} - \frac{d\ln (M/\mathscr{L})_*}{d\ln r} - \frac{d\ln \sigma_v{}^2}{d\ln r}\right], \qquad (11)$$

where $L_*(r)$ and $(M/\mathscr{L})_*(r)$ are respectively the luminosity density and the mass-to-light ratio of the visible stars at radius r. The innermost measurement of σ_v is 350 km s^{-1} at a radius $r = 1''.5 \equiv 110\delta_{15}$ pc from the center of M87. In fact, this value for the central σ_v is too low; it has to be corrected for the contribution from stars in the line of sight in the outer parts of the galaxy. This correction was made by fitting a polynomial function to the observed radial distribution of σ_v and then inverting the appropriate Abel integral. The resulting corrected $\sigma_v = 400$ km s^{-1} was found to be insensitive to the precise polynomial fit. Consequently, we find for the total mass inside $r = 1''.5$:

$$M(1''.5) = 4 \times 10^9\left[-\frac{d\ln L_*}{d\ln r} - \frac{d\ln (M/L)_*}{d\ln r} - \frac{d\ln \sigma_v{}^2}{d\ln r}\right] M_\odot. \qquad (12)$$

In the centers of normal galaxies, which may be represented by isothermal spheres, the logarithmic derivative terms are small or vanish altogether. [Note that near the origin in an isothermal sphere the main term is $(d\ln L_*/d\ln r) \sim -3(r/r_c)^2$; this has the correct behavior at the origin.] In M87, however, the behavior is quite different: by fitting smooth curves through the data we find $(-d\ln \sigma_v{}^2/d\ln r) = 0.6 \pm 0.3$ and $(-d\ln L_*/d\ln r) = 1.0 \pm 0.1$. The logarithmic derivative of $\sigma_v{}^2$ is rather uncertain because of observational scatter, but in any case it is clear that

$(-d \ln \sigma_v^2/d \ln r) > 0$. The value of $(d \ln L_*/d \ln r)$, obtained by correcting the photometric data of Young *et al.* (1978*b*) for projection effects inside the galaxy, is well determined. We recall that there is little evidence, either from broad-band colors or from the behavior of the line strength index γ, for changes in the stellar population in the central regions of M87. For this reason we can neglect the term $[d \ln (M/L)_*/d \ln r]$ in equation (12). We then find $M(r < 1''.5) = (6.5 \pm 1.5) \times 10^9 \delta_{15}\, M_\odot$. Most of the uncertainty in this value lies in the term $(d \ln \sigma_v^2/d \ln r)$ in equation (12). From the photometry we find the total luminosity emitted by the central 1".5 radius to be $V = 14.71 \pm 0.03$ mag. After correction for Galactic absorption $A_v = 0.14$ mag, the total luminosity $\mathscr{L}_P(1''.5) = (2.8 \pm 0.1) \times 10^8 \delta_{15}^2\, L_\odot$. Allowing for projection effects through M87, we find the total brightness inside a sphere of radius 1".5 to be $V = 15.73 \pm 0.07$ mag. Consequently, the luminosity density in the V band is $\mathscr{L}_S(1''.5) = (11.2 \pm 0.8) \times 10^7 \delta_{15}^2\, L_\odot$. Combining this with our earlier mass estimate, we find that the average mass-to-light ratio inside 1".5 is $\langle M/\mathscr{L} \rangle (r < 1''.5) = 58 \pm 16 \delta_{15}^{-1}$ solar units.

We recall that the analysis in § VI led to a value $M/\mathscr{L} \sim 6$ for the stellar population near the center ($r \sim 10''$) of M87. The central value of $M/\mathscr{L}$ is a factor of 10 higher than this and strongly suggests that the nucleus of M87 contains a large, dark central mass. In § VIII we shall return to this point when we calculate the integrated mass-to-light ratio inside r, $\langle M/\mathscr{L} \rangle (r)$, as a function of radius.

b) λ3727 Emission as a Probe of the Central Mass

In Figure 8 we display the [O II] λ3727 emission doublet observed in data set 5 of Table 1. The profile agrees with that observed by Walker and Hayes (1967), and we find widths (after correcting for the instrumental resolution) FWHM [O II] = 600 km s^{-1}, FWZI [O II] = 1500 km s^{-1}. Furthermore, we have determined the emission redshift to be $cz_{em} = 1144 \pm 20$ km s^{-1}, which gives a discrepancy $cz_{ab} - cz_{em} = 143 \pm 30$ km s^{-1}. A similar discrepancy was noted by Humason (quoted in Baade and Minkowski 1954), by Minkowski (1959), and by Walker and Hayes (1967). The latter authors found $cz_{ab} - cz_{em} = 210$ km s^{-1}; however, they took the wavelength of the emission peak which, with their line profile, is ~80 km s^{-1} shortward of the center of luminosity (which we have used).

Walker and Hayes described the structure of the [O II] clouds to consist of (*a*) a broad component contained within the seeing disk ($r \sim 1''$), and (*b*) narrower features protruding out to $r \sim 4''$. Because of their asymmetric profiles, it is likely that the broadening mechanism is simply mass motions of the gas clouds.

We appreciate the dangers of associating the broad lines with gas clouds swirling around a massive object, especially in view of the possibility of ejection or infall. We note, however, that the narrow component has FWHM = 600 km s^{-1}, corresponding to $\sigma = 260$ km s^{-1} at $r \sim 3''$. This is roughly equal to the velocity dispersion found for the stellar population ($\sigma_v = 300$ km s^{-1}) at the same radius. Moreover, the broad component inside $r = 1''$ indicates a central mass $M_N = v^2 r/G = 9.2 \times 10^9 (r_c/1'') \delta_{15}\, M_\odot$, where we have adopted a Keplerian velocity equal to half the FWZI velocity, and r_c is the (unknown) distance of the cloud structures from the center of M87.

In summary, the widths of both components of the λ3727 emission line are entirely consistent with the

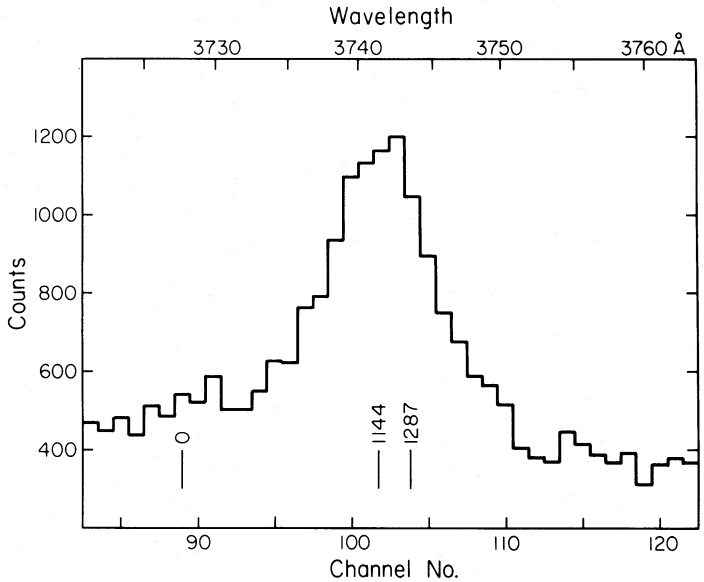

FIG. 8.—The [O II] λ3727 doublet in the nucleus of M87. The vertical markers give the rest wavelength ($v = 0$ km s^{-1}), the redshift of the center of luminosity of the [O II] lines ($v = 1144$ km s^{-1}), and the stellar absorption redshift of M87 ($v = 1287$ km s^{-1}).

hypothesis that the emitting gas is contained by a central mass of the order of that found from our earlier considerations.

VIII. DETERMINATION OF $\langle M/\mathscr{L}\rangle$ AS A FUNCTION OF RADIUS

To solve the problem of the determination of $(M/\mathscr{L})(r)$, we consider the equation of stellar hydrodynamics,

$$\frac{d}{dr}[\rho(r)\sigma_v^2(r)] = \frac{4\pi G\rho(r)}{r^2}\int_0^r s^2\rho(s)ds\,, \qquad (13)$$

where $\sigma_v^2(r)$ is a given, observed function of r. (Note that we have again assumed isotropy of σ_v and spherical symmetry for the galaxy.) This equation can be solved in principle to give $\rho(r)$, given $\sigma_v(r)$. The luminosity profile $L(r)$ can be determined from the surface photometry; the ratio $\rho(r)/L(r)$ then gives $(M/\mathscr{L})(r)$. In practice, the data for $\sigma_v(r)$ are subject to a scatter of about 10%. The solution of equation (13) ultimately involves differentiating an empirical function and is therefore impracticable. Instead, we shall adopt an integral approach which determines the mean $M/\mathscr{L}$ contained within a given radius, denoted $\langle M/\mathscr{L}\rangle(r)$. This method is less sensitive to the errors but is adequate to detect changes by a factor of 2 in $M/\mathscr{L}$. We compute:

$$M(r) = \frac{r\sigma_v^2(r)}{G}\left[-\frac{d\ln L}{d\ln r} - \frac{d\ln \sigma_v^2}{d\ln r}\right], \qquad (14)$$

which again neglects the (probably small) logarithmic derivative $[d\ln(M/\mathscr{L})/d\ln r]$. Even if this derivative is of order unity, it will still be outweighed by the term $(d\ln L/d\ln r)$ which is typically -2.3. The derivative $(d\ln\sigma_v^2/d\ln r)$ is found by fitting a smooth curve through the σ_v data points. This will not lead to particularly reliable values because of scatter in the data points, but again we note that this is not critical because $(d\ln L/d\ln r)$ dominates equation (14). This last derivative may be obtained accurately by correcting the surface photometry for projection effects through the galaxy. Our equation for $M(r)$ has the merit that all quantities are locally determined, so that errors at one point r do not propagate catastrophically as they would in solving equation (13) directly. Having obtained $M(r)$, we compute from the photometry

$$\mathscr{L}(r) = 4\pi\int_0^r L(s)s^2ds\,, \qquad (15)$$

and so obtain the ratio $\langle M/\mathscr{L}\rangle(r) = M(r)/\mathscr{L}(r)$.

We first apply this procedure to NGC 3379. The relevant quantities are listed in Table 4 and the results illustrated in Figure 9. As might be expected from the fact that a King model with constant $M/\mathscr{L}$ fits the data, there are no significant radial variations in $\langle M/\mathscr{L}\rangle$.

A similar procedure applied to M87 yields dramatically different results, as may be seen by inspection of Table 5 and Figure 10. The large nuclear mass discussed in §§ VI and VII produces an increase in $\langle M/\mathscr{L}\rangle(r)$ for $r < 10''$ up to a central value of $\langle M/\mathscr{L}\rangle \sim 60$. Outside $r = 10''$, the $\langle M/\mathscr{L}\rangle$ values

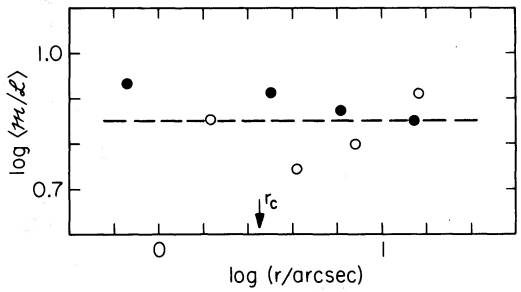

FIG. 9.—Mean mass-luminosity ratio enclosed within radius r $[\langle M/\mathscr{L}\rangle(r)]$ as a function of r in NGC 3379. Open circles (○) are to the S, and filled circles (●) are to the N of the center. The core radius of the galaxy, $r_c = 2''.8$, is marked.

TABLE 4

RADIAL DEPENDENCE OF $(M/\mathscr{L})$ FOR NGC 3379

Radius (arcsec)	σ_v (observed) (km s^{-1})	σ_v† (deprojected) (km s^{-1})	$\frac{d\ln\sigma_v^2}{d\ln r}$†	$\frac{d\ln L(r)}{d\ln r}$*	$\frac{M(r)}{10^8\,M_\odot}$	$\frac{\mathscr{L}(r)}{10^8\,L_\odot}$*	$\langle M/\mathscr{L}\rangle(r)$
0.7	223	225	-0.00	-0.18	0.49	0.057	8.6
1.7	206	209	-0.01	-0.80	4.5	0.65	6.9
3.1	214	218	-0.03	-1.75	20	2.5	7.9
4.1	181	186	-0.05	-2.18	22	4.1	5.3
6.5	200	207	-0.09	-2.47	54	7.4	7.3
7.4	188	196	-0.12	-2.56	53	8.7	6.1
13.9	174	186	-0.26	-2.56	103	15.0	6.9
14.2	189	202	-0.26	-2.56	124	15.5	8.0

*Obtained from photometry by Kormendy (1977), and Young et al. (1978c).

†Obtained by fitting a smooth curve through the data points in Table 3.

TABLE 5

RADIAL DEPENDENCE OF $(M/\mathscr{L})$ FOR M87

Radius (arcsec)	σ_v (observed) (km s^{-1})	$\sigma_v^{\dagger}$ (deprojected) (km s^{-1})	$\frac{d \ln \sigma_v^2}{d \ln r}^{\dagger}$	$\frac{d \ln L(r)}{d \ln r}^{*}$	$\frac{M(r)}{10^{10} M_\odot}$	$\frac{\mathscr{L}(r)}{10^{10} L_\odot}^{*}$	$\langle M/\mathscr{L} \rangle(r)$
1.6	329	395	-0.62	-1.01	0.66	0.011	60
2.2	362	423	-0.50	-0.94	0.94	0.015	63
3.2	321	360	-0.40	-0.87	0.86	0.029	30
3.8	333	367	-0.36	-0.88	1.04	0.040	26
9.2	295	310	-0.26	-1.43	2.45	0.22	11.1
9.7	301	317	-0.25	-1.45	2.72	0.24	11.3
9.7	286	301	-0.25	-1.45	2.45	0.24	10.2
11.3	275	287	-0.25	-1.66	2.92	0.32	9.1
22.1	260	269	-0.09	-2.27	6.20	0.92	6.7
22.7	280	290	-0.09	-2.27	7.40	0.93	7.9
24.3	287	297	-0.10	-2.28	8.37	1.0	8.1
41.6	268	283	-0.18	-2.29	13.5	1.9	7.2
62.6	258	276	-0.29	-2.30	20.3	2.7	7.4
69.7	189	203	-0.33	-2.30	12.4	3.0	4.2
71.8	232	250	-0.35	-2.30	19.5	3.1	6.4

*Obtained from CCD photometry by Young et al. (1978b).

†Obtained by fitting a smooth curve to the data points of Table 3 and Figure 4.

are roughly those found earlier for the stellar population in M87 (with $M/\mathscr{L} = 6$). Since a King model with $M/\mathscr{L}$ = constant fits the data for the outer regions of M87, we do not expect any significant rise in $M/\mathscr{L}$ at large radii; this expectation is confirmed in Figure 10.

We have found no evidence for an increase in $M/\mathscr{L}$ at large radii, and thus no evidence for massive halos, in NGC 3379 and M87. However, we note that the observations for NGC 3379 and M87 only extend to 5 and 7 core radii, respectively. We were successful in detecting an increase in $M/\mathscr{L}$ at large radii in the elliptical galaxy NGC 4473 (Young *et al.* 1978*a*) where observations extended to 14 core radii. Now the equation of hydrostatic equilibrium has the power law solution:

$$\rho = \rho_0 \left(\frac{r_0}{r}\right)^{k+2};$$

$$\sigma_v^2(r) = \frac{2\pi}{1-k^2} G\rho_0 r_0^2 \left(\frac{r_0}{r}\right)^k \quad (|k| < 1). \qquad (16)$$

Since the luminosity profile $L(r)$ has a typical gradient $(d \ln L/d \ln r) = -2.30$ in the outer regions of a galaxy, an observation that $k = -(d \ln \sigma_v^2/d \ln r) < 0.3$ would suggest that $M/\mathscr{L}$ ultimately increases with radius.

IX. CONCLUSIONS

a) *Summary of the Measurements*

We have used the IPCS detector working in a fully two-dimensional mode in order to determine the radial variation of radial velocity cz, line strength γ, and velocity dispersion σ_v in the elliptical galaxies M87 and NGC 3379. Values of these parameters were derived from the observed spectra by an application of the Fourier method described by SSBS. The main conclusions are as follows:

1. NGC 3379 exhibits a slight rotation from observations made in P.A. 0° (the major axis is at P.A. 68°). The semiamplitude is 4.0 ± 1.3 km s^{-1} arcsec^{-1} when corrected to the major axis. The line strength and σ_v decrease slightly with increasing radius.

2. The mean photometric profile of NGC 3379 and the measurements of σ_v (observed out to $r = 14''$) are both adequately fitted by a King (1966) model with $\log r_T/r_c = 2.20$ and $M/\mathscr{L} = (6 \pm 1)(\Delta_{\rm Mpc}/8)^{-1}$, where $\Delta_{\rm Mpc}$ is the distance in Mpc. Overall, there is no evidence in NGC 3379 for an increase in $M/\mathscr{L}$ with radius. However, the observations extend out to only 5 core radii.

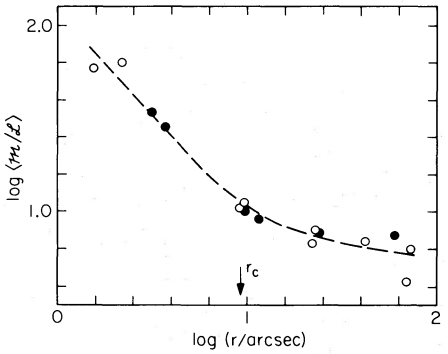

FIG. 10.—Mean mass-luminosity ratio enclosed within radius r $[\langle M/\mathscr{L} \rangle(r)]$ as a function of r in M87. Open circles (○) are to the W of the nucleus, and filled circles (●) are to the E. The core radius of the galaxy, $r_c = 9\farcs6$, is marked.

3. In M87 the amplitude of any rotation is less than 10 km s^{-1} along an E-W axis for $r \leq 72''$. The line strength index is sensibly constant inside the core radius $r_c = 9''.6$, but then falls off with increasing radius. The velocity dispersion shows a complex behavior; σ_v rises slowly from about 220 km s^{-1} at $r = 72''$ to $\sigma_v = 280$ km s^{-1} at $r = r_c$. It then rises rapidly with decreasing r, reaching a maximum measured value of $\sigma_v = 350$ km s^{-1} at $r = 1''.5$.

4. The photometric profile and the radial run of σ_v in M87 are adequately fitted by a King model with $\log r_T/r_c = 2.10$ for $20'' < r < 72''$. The value of $M/\mathscr{L}$ in these outer regions is $6.5 \pm 0.6\,(\Delta_{\rm Mpc}/15)^{-1}$ solar units, where $\Delta_{\rm Mpc}$ is the distance in Mpc. As in the case of NGC 3379, there is no evidence from our data for an increase in $M/\mathscr{L}$ with increasing radius in M87.

5. The sharp increase in σ_v inside the core radius in M87, combined with the photometric data of Young *et al.* (1978*b*), leads to the conclusion that $\langle M/\mathscr{L}\rangle$ increases rapidly as $r \to 0$. We showed quantitatively in §§ VI, VII, and VIII, by different approaches, that the value of $M/\mathscr{L}$ in the central $1''.5$ radius is about 60 solar units, despite the fact that the quality of the stellar population (as indicated by the line strength index γ) remains sensibly constant with radius. The data imply that M87 contains a central, dark mass of about $5 \times 10^9\ M_\odot$ inside $r = 110\delta_{15}$ pc.

b) Discussion

In their outer regions the two galaxies M87 and NGC 3379 behave quite similarly. The photometric and dynamical measurements are consistent with King models and there is no sign of a massive halo in the form of a gradual outward increase in $M/\mathscr{L}$. In both galaxies our elaborate measurements and methods of analysis have led to a lower value for the mass-to-light ratio ($M/\mathscr{L} \sim 6$) than has been obtained in less complete studies of elliptical galaxies.

In their central regions M87 and NGC 3379 exhibit quite different properties. In the case of NGC 3379 the data are fitted tolerably by the same King model which fits the outer regions. In M87 an additional dark central mass must be added to the King model. We estimated that $5 \times 10^9\ M_\odot$ must be concentrated in a volume less than $110\delta_{15}$ pc in radius. It is not possible to prove from our data that this object is a black hole. However, the fact that as we approach the center of M87 the stellar population, as adduced from the spectral lines, does not change its gross character whereas the value of $\langle M/\mathscr{L}\rangle$ rises markedly implies to us that the presence of a central, supermassive black hole must be a serious possibility. It is easy to imagine high-resolution spectroscopic and photometric observations which could be carried out with the Space Telescope to further test this hypothesis.

We are extremely grateful to the many members of the Kitt Peak staff who made the special arrangements required for these observations. We also thank J. Fordham for his assistance with the IPCS. We especially thank Jim Westphal, Jerry Kristian, Chris Wilson, and Fred Landauer for the close cooperation involved in analyzing the M87 data presented in this and the accompanying paper. W. S. thanks the National Science Foundation for support under grant AST 75-00555. The work at University College London was supported by grants from the UK Science Research Council. We also thank Peter Goldreich, Scott Tremaine, and Paul Schechter for invaluable discussions.

REFERENCES

Baade, W., and Minkowski, R. 1954, *Ap. J.*, **119**, 215.
Bertola, F., and Capaccioli, M. 1975, *Ap. J.*, **200**, 439.
Boksenberg, A., and Sargent, W. L. W. 1975, *Ap. J.*, **198**, 31.
Brandt, J. C., and Roosen, R. G. 1969, *Ap. J. (Letters)*, **156**, L59.
Burbidge, E. M., Burbidge, G. R., and Fish, R. A. 1961, *Ap. J.*, **134**, 251.
Dennison, E. W. 1954, thesis, University of Michigan (unpublished).
de Vaucouleurs, G. 1959, in *Handbuch der Physik*, ed. S. Flügge (Berlin-Götingen-Heidelberg: Springer-Verlag), **53**, 311.
———. 1974, in *IAU Symposium No. 58, The Formation and Dynamics of Galaxies*, ed. J. R. Shakeshaft (Dordrecht: Reidel), p. 1.
———. 1975, in *Stars and Stellar Systems*, Vol. **9**, ed. A. Sandage, M. Sandage, and J. Kristian (Chicago: University of Chicago Press), p. 557.
de Vaucouleurs, G., and Capaccioli, M. 1978, in preparation.
de Vaucouleurs, G., de Vaucouleurs, A., and Corwin, H. G., Jr. 1976, *Second Reference Catalogue of Bright Galaxies* (Austin: University of Texas Press).
Faber, S. M., and Jackson, R. E. 1976, *Ap. J.*, **204**, 668.
King, I. R. 1966, *A.J.*, **71**, 64.
Kormendy, J. 1977, *Ap. J.*, **214**, 359.
Minkowski, R. 1959, in *IAU Symposium No. 9, Paris Symposium on Radio Astronomy*, ed. R. N. Bracewell (Stanford: Stanford University Press), p. 335.
———. 1962, in *IAU Symposium No. 15, Problems of Extragalactic Research*, ed. G. C. McVittie (New York: Macmillan), p. 112.
Sandage, A. R., and Tammann, G. A. 1974, *Ap. J.*, **194**, 559.
Sargent, W. L. W., Schechter, P. L., Boksenberg, A., and Shortridge, K. 1977, *Ap. J.*, **212**, 326 (SSBS).
Walker, M. F., and Hayes, S. 1967, *Ap. J.*, **149**, 481.
Williams, T. B. 1977, *Ap. J.*, **214**, 685.
Young, P. J, Sargent, W. L. W., Boksenberg, A., Lynds, C. R., and Hartwick, F. D. A. 1978*a*, preprint.
Young, P. J, Westphal, J. A., Kristian, J. A., Wilson, C. P., and Landauer, F. 1978*b*, *Ap. J.*, **221**, in press.
———. 1978*c*, in preparation.

A. Boksenberg and Keith Shortridge: Department of Physics and Astronomy, University College London, Gower Street, London WC1E 6BT, England

F. D. A. Hartwick: Department of Astronomy, University of Victoria, Victoria V8W 2Y2, B.C., Canada

C. R. Lynds: Kitt Peak National Observatory, P.O. Box 26732, Tucson, AZ 85726

W. L. W. Sargent and Peter Young: Department of Astronomy 105-24, California Institute of Technology, Pasadena, CA 91125